

Impairment of bidirectional synaptic plasticity in the striatum of a mouse model of DYT1 dystonia: role of endogenous acetylcholine

Giuseppina Martella,^{1,*} Annalisa Tassone,^{2,*} Giuseppe Sciamanna,² Paola Platania,¹ Dario Cuomo,² Maria Teresa Viscomi,² Paola Bonsi,² Emanuele Cacci,^{3,4} Stefano Biagioni,^{3,4} Alessandro Usiello,^{5,6} Giorgio Bernardi,^{1,2} Nutan Sharma,⁷ David G. Standaert⁸ and Antonio Pisani^{1,2}

1 Department of Neuroscience, University "Tor Vergata", 00133 Rome, Italy

2 Fondazione Santa Lucia I.R.C.C.S., Rome, Italy

3 Department of Cell and Developmental Biology, Neurobiology Research Unit, University "La Sapienza", Rome, Italy

4 "Daniel Bovet" Neurobiology Research Center, University "La Sapienza", Rome, Italy

5 CEINGE Biotechnologie Avanzate, Naples, Italy

6 Department of Health Sciences, University of Molise, Italy

7 Massachusetts General Hospital, Harvard Medical School, Boston, USA

8 University of Alabama at Birmingham, Birmingham, USA

*These authors contributed equally to this work.

Correspondence to: Antonio Pisani, MD,
Department of Neuroscience,
University "Tor Vergata",
00133 Rome,
Italy
E-mail: pisani@uniroma2.it

Correspondence may also be addressed to: David G. Standaert, MD, PhD,
University of Alabama at Birmingham,
Birmingham, USA
E-mail: dstandaert@uab.edu

DYT1 dystonia is a severe form of inherited dystonia, characterized by involuntary twisting movements and abnormal postures. It is linked to a deletion in the *dyt1* gene, resulting in a mutated form of the protein torsinA. The penetrance for dystonia is incomplete, but both clinically affected and non-manifesting carriers of the DYT1 mutation exhibit impaired motor learning and evidence of altered motor plasticity. Here, we characterized striatal glutamatergic synaptic plasticity in transgenic mice expressing either the normal human torsinA or its mutant form, in comparison to non-transgenic (NT) control mice. Medium spiny neurons recorded from both NT and normal human torsinA mice exhibited normal long-term depression (LTD), whereas in mutant human torsinA littermates LTD could not be elicited. In addition, although long-term potentiation (LTP) could be induced in all the mice, it was greater in magnitude in mutant human torsinA mice. Low-frequency stimulation (LFS) can revert potentiated synapses to resting levels, a phenomenon termed synaptic depotentiation. LFS induced synaptic depotentiation (SD) both in NT and normal human torsinA mice, but not in mutant human torsinA mice. Since anti-cholinergic drugs are an effective medical therapeutic option for the treatment of human dystonia, we reasoned that an excess in endogenous acetylcholine could underlie the synaptic plasticity impairment. Indeed, both LTD and SD were rescued in mutant human torsinA mice

either by lowering endogenous acetylcholine levels or by antagonizing muscarinic M_1 receptors. The presence of an enhanced acetylcholine tone was confirmed by the observation that acetylcholinesterase activity was significantly increased in the striatum of mutant human torsinA mice, as compared with both normal human torsinA and NT littermates. Moreover, we found similar alterations of synaptic plasticity in muscarinic M_2/M_4 receptor knockout mice, in which an increased striatal acetylcholine level has been documented. The loss of LTD and SD on one hand, and the increase in LTP on the other, demonstrate that a 'loss of inhibition' characterizes the impairment of synaptic plasticity in this model of DYT1 dystonia. More importantly, our results indicate that an unbalanced cholinergic transmission plays a pivotal role in these alterations, providing a clue to understand the ability of anticholinergic agents to restore motor deficits in dystonia.

Keywords: dystonia; synaptic plasticity; striatum; acetylcholine; electrophysiology

Abbreviations: ACh = acetylcholine; AChE = acetylcholinesterase; HFS = high-frequency stimulation; hMT = mutant human torsinA; hWT = normal human torsinA; LFS = low-frequency stimulation; LTD = long-term depression; LTP = long-term potentiation; MSN = medium spiny neuron; NT = non-transgenic; PPR = paired-pulse ratio; SD = synaptic depotentiation; RMP = resting membrane potential

Introduction

Dystonia is a neurological syndrome of involuntary muscle contractions, causing twisting, repetitive movements and progressive abnormal postures (Fahn, 1988). DYT1 dystonia is the most common form of inherited early-onset generalized dystonia. It is caused by a 3 bp deletion that deletes a glutamic acid residue in the C-terminal coding region of the protein torsinA (Ozelius *et al.*, 1997). The physiological function of torsinA is unclear, but it has sequence homology to the family of 'ATPases associated with a variety of cellular activities' (AAA+ proteins), which perform chaperone-like functions and assist in protein trafficking, membrane fusion and in secretory processing (Goodchild *et al.*, 2005; Hewett *et al.*, 2007; Breakefield *et al.*, 2008; Granata *et al.*, 2008). Pathologically, there is no clear evidence for neural degeneration in the few human post-mortem cases of DYT1 dystonia that have been examined, suggesting that functional and/or ultrastructural alterations, rather than neurodegenerative processes underlie the dystonic symptoms (Rostasy *et al.*, 2003). A growing body of evidence suggests that the DYT1 mutation produces dystonia through aberrant neuronal signalling within the basal ganglia, and more specifically in the striatum (Todd and Perlmutter 1998; Rostasy *et al.*, 2003; Breakefield *et al.*, 2008). Over-activation of the basal ganglia circuits is observed in many forms of dystonia (Ceballos-Baumann and Brooks, 1997; Playford *et al.*, 1998). In DYT1 dystonia, abnormal motor plasticity has been reported (Edwards *et al.*, 2006), while clinically unaffected DYT1 gene carriers have subtle abnormalities in motor behaviour with impaired sequence learning (Ghilardi *et al.*, 2003). Therefore, altered motor plasticity appears to play a relevant role in the pathophysiology of dystonia. Although mouse models of DYT1 dystonia do not exhibit overt dystonia, they do display abnormalities of motor learning, reminiscent of the human non-manifesting carrier state (Sharma *et al.*, 2005; Breakefield *et al.*, 2008).

Long-term changes in synaptic efficacy at corticostriatal synapses are thought to be the cellular basis of motor learning and associative memory processes. High-frequency stimulation (HFS) of glutamatergic striatal afferents can induce either long-term depression (LTD) or long-term potentiation (LTP) at this synapse (Calabresi *et al.*, 1992a, b; Lovinger *et al.*, 1993), depending

on a variety of complex signalling mechanisms (Kreitzer and Malenka, 2008; Shen *et al.*, 2008). Nevertheless, compelling evidence suggests that cholinergic transmission is a major modulator of the induction process (Wang *et al.*, 2006; Bonsi *et al.*, 2008). Despite the intrinsic nature of acetylcholine (ACh) innervation, cholinergic interneurons profoundly influence synaptic activity and plasticity of medium spiny neurons (MSNs) (Pisani *et al.*, 2007). Recently, we have identified a profound alteration of cholinergic function in transgenic mice that over-express mutant torsinA (hMT mice). In cholinergic interneurons, the normal response to activation of dopamine D2 receptors is inhibition of firing activity. In hMT mice, we observed instead a paradoxical excitatory response, which likely results in an enhanced acetylcholine release (Pisani *et al.*, 2006). Hence, in the present work, we investigated the possibility that an unbalanced cholinergic tone could disrupt synaptic plasticity in this mouse model of DYT1 dystonia. Using a combination of electrophysiological, morphological, biochemical and molecular approaches, we examined glutamatergic synaptic plasticity in slices from either hMT mice or mice expressing human wild-type torsinA (hWT). Our results demonstrate a substantial alteration of corticostriatal synaptic plasticity in hMT mice. More importantly, they show that normalizing striatal cholinergic signalling fully restores physiological synaptic plasticity.

Materials and Methods

Transgenic mice and genotyping

Treatment and handling of animals was carried out in accord with both the EC and Italian guidelines (86/609/EEC; D.Lvo 116/1992, respectively) and approved by the University of Rome 'Tor Vergata' (n. 153/2001A). Transgenic mice (8- to 10-weeks old) were generated as previously described (Sharma *et al.*, 2005). Breeding colonies of both hWT and hMT mice were established at our animal house. For each strain, non-transgenic (NT) littermates were utilized as controls, and are defined as NT mice (C57BL-6). Hence, the genetic background was identical between the control and experimental animals, with the only difference being the presence of the transgene. Age-matched

muscarinic M_2/M_4 knockout ($^{-/-}$) mice were generated as described (Duttaroy *et al.*, 2002); wild-type littermates of the same mixed genetic background were utilized as controls.

For genotyping, tail DNA from mice was isolated using the Extract-N-Amp Tissue PCR Kit (Catalogue Numbers XNAT2, Sigma-Aldrich, Italy). To amplify a 560 bp segment, two specific primers for human torsinA were utilized (5'-CACATTGCACCTTCCACATGCT-3' and 5'-GTTTTGCAGCCTTATCTGA-3'). The samples were prepared according to the 'Tissue Preparation' and 'Reagent Preparation' protocols (Sigma-Aldrich; 35 cycles; annealing temperature 60°C). The human torsinA coding sequence was identified via 1.5% agarose gel electrophoresis. The mouse genotype was confirmed by restriction digestion with BseRI (New England BioLabs, USA). The human torsinA and human mutant torsinA PCR products were digested with BseRI into different fragments (279, 238, 24, 22 and 279 bp; 259 and 22 bp, respectively). Then, fragment profiles were identified by gel electrophoresis, using 2% SYBR Safe agarose (Invitrogen, Italy) (Fig. 1A).

Tissue slice preparation

Mice were sacrificed by cervical dislocation under ether anaesthesia and the brain was immediately removed from the skull. Coronal corticostriatal slices (250–300 μm thick; Fig. 1C) were cut with a vibratome in Krebs' solution (126 NaCl, 2.5 KCl, 1.3 MgCl_2 , 1.2 NaH_2PO_4 , 2.4 CaCl_2 , 10 glucose, 18 NaHCO_3 , all expressed in millimolars), bubbled with 95% O_2 and 5% CO_2 . In another set of experiments, parasagittal slices (300 μm) were prepared as described in detail previously (Fig. 1E; Smeal *et al.*, 2007; Ding *et al.*, 2008). In these slices (cut at 9–10°C), a knife-cut was made between the striatum and the thalamus, to prevent contamination from thalamostriatal inputs (Ding *et al.*, 2008). After 30–60 min recovery, individual slices were transferred into a recording chamber (~0.5–1 ml volume), continuously superfused with oxygenated Krebs' medium, at 2.5–3 ml/min and maintained constantly at 32–33°C.

Electrophysiology

Current-clamp recordings were performed blindly using sharp micro-electrodes filled with 2 M KCl (40–60 $\text{M}\Omega$). This electrophysiological approach was used to retain the fidelity of post-receptor signalling pathways. Signal acquisition and off-line analysis were performed with an Axoclamp 2B amplifier and pClamp9 software (Molecular Devices, USA). Striatal neurons were characterized according to their peculiar electrophysiological properties (Table 1). Glutamatergic excitatory post-synaptic potentials (EPSPs) were evoked with a bipolar electrode placed either in the corpus callosum (coronal slices) or in the cortex (V–VI layer, parasagittal slices, Fig. 1C and E), to activate glutamatergic afferents, and were recorded in the presence of bicuculline (10 μM) to prevent GABA_A -receptor contamination. Stimuli of increasing intensity (50–500 μA , 30 μs duration, Fig. 2) were delivered at 0.1 Hz and six traces were averaged at each stimulus intensity. Then, peak excitatory post-synaptic potential amplitudes were measured and input–output relationships were obtained (pClampfit 9.2 software). The averaged excitatory post-synaptic potential whose peak amplitude was 50% of the maximum was further analysed for comparison among genotypes. Paired-pulse facilitation was assessed by presenting two stimuli, which evoked synaptic responses at ~50% of maximal amplitude, with an interstimulus interval of 50 ms and measuring the ratio of the peak amplitude of the second excitatory post-synaptic potential (EPSP2), divided by the first (EPSP1). For HFS (three trains: 3 s duration, 100 Hz frequency, 20 s intervals),

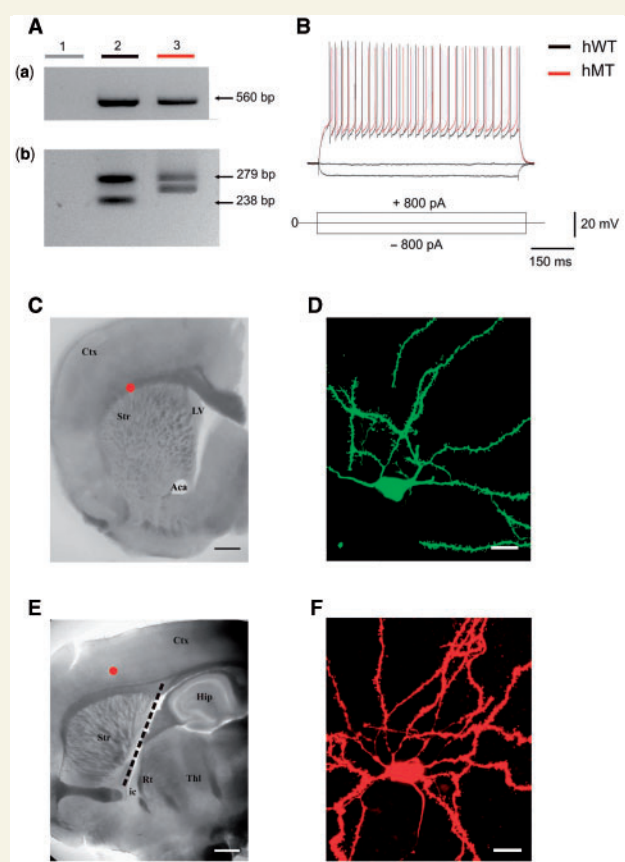


Figure 1 Mouse genotyping and characterization of medium spiny neurons. (A) Analysis of NT, hWT and hMT mice genotype. Representative gel images of PCR products before (a) and after (b) digestion are shown. Products from hWT and hMT mice appear in lanes 2 and 3. Lane 2 shows two major fragments of 279 and 238 bp; lane 3 shows an identical fragment of 279 bp, and a different fragment of 259 bp. Note, in NT mice, the absence of human torsinA (lane 1). (B) Superimposed traces showing voltage responses to current steps (800 pA, 700 ms) in both depolarizing and hyperpolarizing direction in a MSN recorded from either hWT (black trace; RMP = -81 mV) or hMT (red trace; RMP = -78 mV) mice. The long depolarizing ramp to spike threshold, as well as the strong inward rectification during hyperpolarizing steps are peculiar features of striatal spiny neurons. (C and E) Light micrographs of a corticostriatal coronal and parasagittal slice preparation, respectively. Scale bars: 800 μm . Red dots indicate where the stimulating electrode was positioned. In E, dotted lines indicate the site where a knife cut was made between the striatum and the thalamus, to prevent contamination from thalamostriatal inputs. (D and F) Confocal microscope images of biocytin-loaded medium spiny neurons, recorded from coronal (D) or parasagittal (F) slices from hMT mice. Note the branched dendrites densely embedded with spines. Scale bar: 20 μm . Ctx = cortex; Str = striatum; Rt = reticular nucleus of the thalamus; Hip = hippocampus; ic = internal capsula; aca = anterior commissure, anterior; LV = lateral ventricle; Thl = thalamus.

Table 1

MSN	Membrane properties				Statistics				
	NT (a)	hWT (b)	HMT (c)	$M_2/M_4^{-/-}$ (d)	(a) versus (b)	(a) versus (c)	(a) versus (d)	(b) versus (c)	(c) versus (d)
RMP (mV)	86.1 ± 3.3	85.4 ± 4.2	89.1 ± 5.1	84.1 ± 6.2	0.3	0.3	0.3	0.2	0.2
Ri (MΩ)	32.4 ± 5.2	34.6 ± 4.1	33.7 ± 5.6	32.6 ± 4.4	0.7	0.8	0.7	0.9	1
Firing elicited by depolarizing current	Tonic	Tonic	Tonic	Tonic					
Action potential amplitude (mV)	62.7 ± 7.9	61.5 ± 8.4	63.9 ± 9.7	61.2 ± 7.4	1	0.9	0.9	0.9	0.8
Action potential duration (ms)	34.8 ± 5.4	37.2 ± 4.2	36.4 ± 6.2	36.1 ± 5.6	0.7	0.6	0.7	0.9	0.8
Delay to first spike (ms)	44.1 ± 2.2	41.6 ± 5.9	40.6 ± 7.1	42 ± 4.1	0.2	0.5	0.4	0.2	0.4

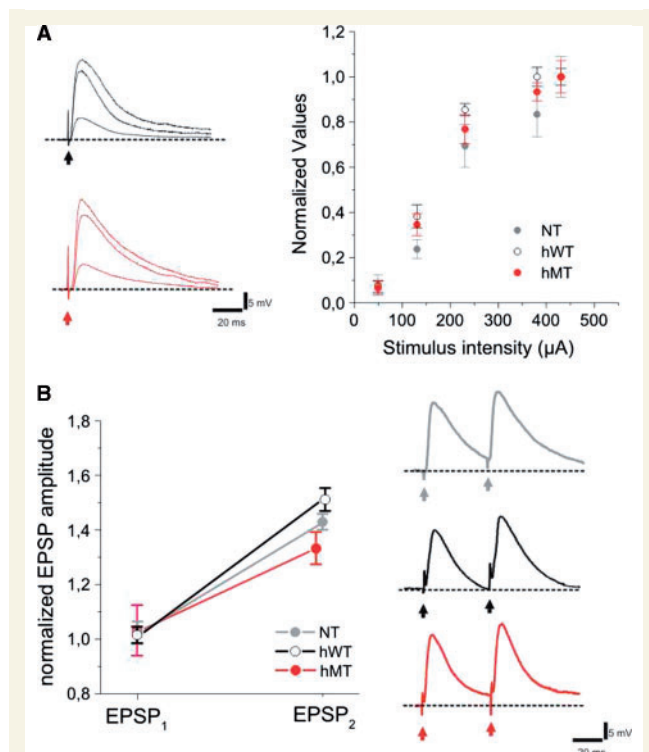


Figure 2 Synaptic properties of the recorded cells. (A) EPSPs evoked by cortical stimulation (arrow indicates the time of synaptic stimulation). The superimposed traces show no differences between hWT and hMT (lower traces) at the three different stimulation intensities (indicated in the graph). The graph shows the normalized input–output relationship measured in the NT (grey circles), hWT (open circles) and hMT (red circles) mice. Circles represent the three different intensities of the stimulation needed to evoke the EPSPs of increasing amplitude in MSNs of the three genotypes. No statistically significant difference was measured among groups. (B) Paired-pulse facilitation (50 ms interstimulus interval) is preserved in both hWT and hMT mice as compared with NT neurons. (Right) Representative paired recordings of EPSPs measured from MSNs from the three distinct groups of mice. Each data point in the plot is the mean ± SEM of at least six independent recordings.

stimulus intensity was raised to spike threshold level. The amplitude of EPSP was averaged and plotted as percentage of the control amplitude for ~10 min pre-high-frequency stimulation. Magnesium (Mg^{2+}) was omitted from the perfusing solution to relieve the Mg^{2+} -dependent block of NMDA receptors, a procedure required during sharp-microelectrode recordings to optimize LTP induction (LTP protocol) (Calabresi *et al.*, 1992b). Synaptic depotentiation (SD) was induced by a low-frequency stimulation (LFS) protocol (2 Hz, 10 min), applied 20–30 min after LTP induction. One to six neurons per animal were recorded, each electrophysiological measure in the three groups of mice was obtained by pooling data from at least four distinct animals. One cell per slice was used for synaptic plasticity experiments.

Parasagittal hippocampal slices (300–400 µm) were prepared as previously described (Errico *et al.*, 2008). Extracellular field excitatory post-synaptic potentials (fEPSPs) were recorded in stratum radiatum of the area CA1. The recording electrode [glass microelectrodes filled with artificial cerebral spinal fluid (ACSF)] was placed in the pyramidal cell layer of CA1 and a bipolar electrode was placed in stratum radiatum to activate the Schaeffer collaterals. Data were filtered at 3–10 kHz using an Axoclamp 2B Amplifier (Molecular Devices, USA), and collected for online analysis at a sampling rate of 20 kHz using LTP software (Anderson and Collingridge, 2007). The slope of the initial rising phase of the fEPSP was used as a measure of synaptic efficacy and the stimulus intensity was set to give a basal response with slope measurement ~40% of that at which a population spike was first observed. All data were normalized to the baseline preceding the HFS protocol (1 train, 100 Hz, 1 s). Data are expressed as mean ± SEM. Statistical significance was assessed using the Student's *t*-test. Drugs were from Tocris Cookson (UK), except for muscarine, trihexyphenidyl, hemicholinium-3 and bicuculline (Sigma Aldrich, Italy), and were applied by switching the control perfusion to drug-containing solution.

Histology and immunohistochemistry

Histological samples were obtained both from perfused animals and biocytin-loaded slices from the three groups of mice: NT, hWT and hMT. Mice were group-housed in standard cages and kept under a 12 h light/dark cycle in a conditioned facility. Food and water were provided *ad libitum*. The animals were transcardially perfused under deep anaesthesia (ketamine and xylazine, 0.2 ml/10 g body weight, i.p.) with 150 ml of 0.9% saline at room temperature (RT) followed by 200 ml of cold 4% paraformaldehyde in 0.1 M pH 7.4 phosphate buffer (PB). Brains were dissected, post-fixed for 2 h at RT and cryo-protected in 30% PB/sucrose at 4°C. They were then frozen with dry

ice and cut into 40 μm -thick transverse sections with a freezing microtome. Randomly, recording electrodes were also loaded with 2% biocytin to examine the morphology of the recorded neurons. Immediately after recording, slices containing biocytin-loaded cells were fixed by immersing in 4% paraformaldehyde in 0.1 M PB overnight at +4°C. The slices were subsequently immersed in 30% PB/sucrose at 4°C. They were then frozen with dry ice and cut into 35 μm -thick transverse sections. Sections derived from biocytin-loaded slices were immediately incubated with Cy2- or Cy3-conjugated Streptavidin (1:200; Jackson ImmunoResearch, Laboratories, USA) in PB 0.3% Triton X-100 for 1 h at RT. Sections derived from perfused animals were incubated with a solution containing rabbit anti-dopamine and cAMP regulated phosphoprotein (DARPP)-32 (1:200; Millipore, cat. number AB1656, Billerica, USA), mouse anti-torsinA (1:300, Cell Signalling, USA), guinea pig anti-Substance P (SP, 1:200, Abcam, UK) primary antibodies in PB 0.3% Triton X-100 overnight at +4°C. After three washes in PB, sections were incubated with a solution containing a Cy2-conjugated donkey anti-mouse, Cy3-conjugated donkey anti-rabbit, Cy5-conjugated donkey anti-guinea pig IgGs (1:200; Jackson ImmunoResearch, Laboratories) secondary antibodies. After three washes in PB, sections derived from all histological material were mounted on slides, air-dried and coverslipped with GEL MOUNT (Biomedica, USA). Fluorescence was examined under a confocal scanning laser microscope (CSLM Leica SP5, Leica Microsystems, Germany). Final images were projections of z-stack series taken through a total thickness of 20 μm . Figures were generated by adjusting only brightness and contrast, and composed by using Adobe Illustrator 10. After a visual inspection of the labelling throughout the sections, all images were acquired from the dorso-lateral striatal region where recordings were performed.

The quantitative analysis of double immunolabelled neurons was performed on digital images acquired through CLSM using a 40X objective at a 0.7 zoom factor. Three separate fields (dorso-lateral, central, medial) in three digital squared frames (200 μm per side) of five rostro-caudally spaced sections were examined ($n=5$ animals).

Cellular co-localization of double-labelled neurons was analysed by counting and characterizing cell labelling off-line through the CLSM proprietary image analysis programme. The features of immunolabelled neurons were analysed by zooming on the cells and by serially excluding each channel. Double- and single-immunolabelled neurons were then digitally marked, recorded and the material was stored in a data archive. All data were expressed as mean \pm SEM.

Western blotting

NT, hWT and hMT mice ($n=8$ per genotype) were killed and the striata dissected out, sonicated in 200 μl of 1% sodium dodecyl sulfate (SDS) and boiled for 10 min. Equal amounts of total protein (30 μg) from each sample were loaded onto 10% polyacrylamide gels. Proteins were separated, transferred and membranes immunoblotted as described earlier (Errico *et al.*, 2008). Selective antibodies against NR1 (1:1000; Sigma, St Louis, MO, USA), NR2A (1:1000; Sigma), NR2B (1:1000; Upstate, Lake Placid, NY, USA), GluR1 (1:5000; Chemicon, Temecula, CA), GluR2/3 (1:1000; Upstate) and DARPP32 (1:1000; Cell Signaling Technology, Beverly, MA, USA) were used. Blots were then incubated in horseradish peroxidase-conjugated secondary antibodies and target proteins visualized by electrogenerated chemiluminescence (ECL) detection (Pierce, Rockford, IL, USA), followed by quantitation by Quantity One software (Biorad). Optical density values were normalized to DARPP-32 for variations in loading and transfer. Normalized values were then averaged and used for statistical comparisons (Student's *t*-test).

Acetylcholinesterase activity

Striata from NT and both hWT or hMT mice were weighed and homogenized in conical glass/glass homogenizer in a 1:20 w/v ratio. Homogenization was performed in 0.1 M sodium PB pH 7.0 containing 1 M NaCl, 10 mM EDTA, 0.5% Triton X-100, 40 mg/ml leupeptin and 20 mg/ml pepstatin. Cholinesterase extraction was carried out with three cycles of 20 strokes each, with intervening freezing and thawing of the samples. After centrifugation at 12 000 g for 30 min at 4°C, the enzymatic activity was assayed on the supernatant, according to Ellman and coworkers (1961), using 1 mM final concentration of acetylthiocholine iodide as substrate. In order to evaluate the contribution of acetylcholinesterase to the total cholinesterase activity, appropriate inhibitors were also used. Pseudocholinesterase or acetylcholinesterase activity was inhibited by pre-incubating tissue extracts for 1 h with 14 μM ethopropazine or 10^{-5} M BW284c51, respectively. Enzyme activity is expressed as specific activity in units per milligram of protein, 1 U corresponding to 1 μmol of substrate hydrolyzed per min at 30°C, pH 8.0.

Statistical analysis

Electrophysiological results are presented as mean \pm SEM. Student's *t*-test and non-parametric Mann-Whitney test were used to compare means pre- and post-HFS/drug. Analysis of variance (ANOVA) test with a *post hoc* Tukey test were performed among groups ($P<0.05$; $\alpha=0.01$). For all analyses, a $P<0.05$ was considered statistically significant.

Results

Electrophysiological and morphological characterization of MSNs

Passive and active intrinsic membrane properties such as resting membrane potential (RMP), input resistance, action potential amplitude and duration, delay to spike threshold and firing frequency allowed us to identify MSNs. Intrinsic properties of NT MSNs ($n=59$) were not significantly different from those measured from both hWT ($n=62$) and hMT neurons both from coronal and parasagittal slices ($n=76$, 27, respectively) (Table 1), and did not differ from those previously described for mouse MSN in tissue slice preparations (Goldberg *et al.*, 2005; Bonsi *et al.*, 2008). MSNs were silent at rest and depolarizing current pulses caused tonic action potential discharge and strong inward rectification that did not differ among genotypes (Fig. 1B). RMP was kept constant throughout the recording session, by injecting negative current through the recording electrode (0.3–100 pA), whenever required. Membrane potential drift was monitored and subtracted at the end of each recording session. Biocytin labelling confirmed that all the recorded neurons were indeed MSNs with similar appearance among genotypes. Neurons from both coronal and parasagittal slices had medium-sized soma (10–20 μm), an extensive dendritic tree densely studded with spines (Fig. 1D and F).

The immunohistochemical characterization demonstrated that torsinA immunoreactivity was widely distributed throughout the striatal areas examined without apparent variation in the

labelling intensity. The cellular staining was confined to the cytoplasm and sometimes to proximal dendrites of MSNs, as previously shown (Sharma *et al.*, 2005) (Supplementary Fig. S1). We never observed labelling in cell nuclei or fibres. In NT, hWT and hMT mice, torsinA immunostaining was punctate and in the cytoplasm, consistent with localization in the endoplasmic reticulum. On morphological grounds torsinA labelling appeared to be confined to neurons without any evidence of glial labelling. In hMT striata, most of the DARPP-32-positive neurons were also immunoreactive for torsinA ($96.4 \pm 1.9\%$), ruling out the possibility that torsinA expression could be functionally segregated in a specific population of D1- or D2 receptor-containing MSNs (Supplementary Fig. S1). However, not all MSNs expressing DARPP-32 were Substance P (SP)-positive, consistent with the distinct neurochemical profiles of striatal MSNs ($62.8 \pm 0.36\%$). Neurons labelled for torsinA were also DARPP-32 immunoreactive ($89.8 \pm 1.8\%$). This pattern of torsinA expression was common to NT, hWT and hMT mice (data not shown, $P > 0.05$) and is in accordance with the description of a widespread, uniform torsinA labelling of the striatum (Konakova and Pulst, 2001; Walker *et al.*, 2002; Sharma *et al.*, 2005).

Short-term plasticity at glutamatergic synapses

Cortically evoked EPSPs were fully blocked by a combination of N-methyl-D-aspartic acid (NMDA) and α -amino-3-hydroxy-5-methyl-4-isoxazole-propionate (AMPA) glutamate receptor antagonists, Dizocilpine (MK-801; $30 \mu\text{M}$) and 6-cyano-7-nitroquinoxaline-2,3-dione (CNQX; $10 \mu\text{M}$) both in coronal and parasagittal slices. MSNs from NT coronal slices exhibited similar mean amplitude and duration of the EPSPs as compared with MSNs from hWT ($n=16$) and hMT ($n=20$) mice (Fig. 2A; $P > 0.05$). The input–output relationship did not show statistically significant differences among groups (Fig. 2A; ANOVA $P > 0.05$, followed by *post hoc* Tukey test). Paired-pulse facilitation is considered to reliably parallel modifications in transmitter release probability (Schulz *et al.*, 1994). Therefore, we measured

paired-pulse ratio (PPR) as an indicator of pre-synaptic glutamatergic activity. No significant differences in the PPR were found between neurons from NT ($n=11$, 1.36 ± 0.3), hWT ($n=11$, 1.4 ± 0.6) and hMT mice ($n=17$, 1.36 ± 0.06) (Fig. 2B; ANOVA $P > 0.05$).

The absence of possible changes in glutamatergic transmission was further confirmed by our analysis of both NMDA and AMPA receptor subunit expression levels. Indeed, western blotting analysis revealed unchanged expression levels for NMDA and AMPA receptor subunits in both hWT and hMT mice, compared with NT mice (Fig. 3; $P > 0.1$, per each protein; Student's *t*-test).

Selective striatal synaptic plasticity deficits in hMT mice

HFS of glutamatergic afferents led to the induction of robust LTD in MSNs in both coronal and parasagittal slices from NT mice, similar in magnitude and duration to that reported previously in mouse brain slices (Goldberg *et al.*, 2005; Bonsi *et al.*, 2008) (Fig. 4A and B; $51.4 \pm 6.3\%$ of control, from coronal slice, and $51.7 \pm 7.1\%$ from parasagittal slices, measured 25 min post-HFS; $n=34$ and 10, respectively; *t*-test $P < 0.001$ and $P < 0.05$). Similarly, in MSNs from hWT mice, HFS was able to cause an LTD that was indistinguishable from that measured in NT mice (Fig. 4A and B; $50.5 \pm 5.4\%$ and $58.2 \pm 9.7\%$, from coronal and parasagittal slices, respectively, measured 25 min post-HFS; $n=39$ and 6; Mann–Whitney $P < 0.001$). In slices from hMT mice, however, HFS failed to cause any LTD (Fig. 4A and B; $94.9 \pm 7\%$, $n=81$ from coronal slices; LTD was not elicited in 70 cells out of 81; *t*-test $P > 0.05$; $101.4 \pm 10.7\%$, $n=6$ from parasagittal slices, $P > 0.05$).

The LTP induction protocol elicited LTP in NT as well as in hWT mice in both slice preparations (Fig. 4C and D; NT: $151.2 \pm 5\%$ of pre-HFS; 71 out of 84 from coronal slices exhibited LTP; *t*-test $P < 0.0001$; $158.3 \pm 8.1\%$, $n=10$ from parasagittal slices, $P < 0.001$; hWT: $157.1 \pm 2.7\%$, $n=56$, in six cells no LTP was observed, coronal slices; *t*-test $P < 0.0001$; $162.5 \pm 13.1\%$, $n=5$ from parasagittal slices, $P < 0.0001$). Notably, in MSNs from

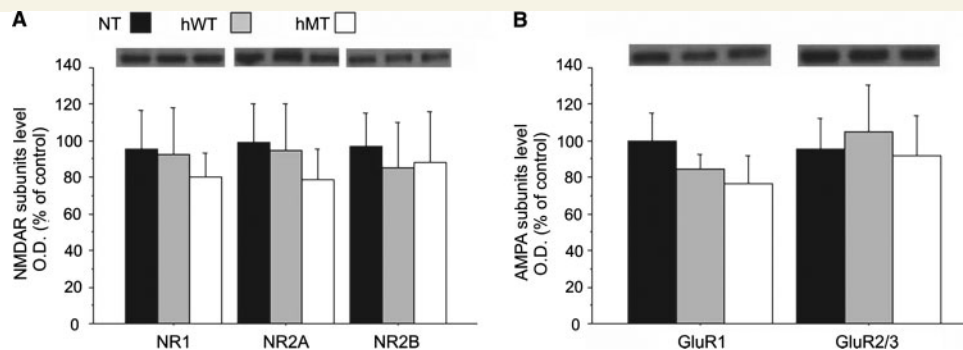


Figure 3 NMDA and AMPA receptor subunit expression. hWT and hMT mice display unaltered levels of the NMDA and AMPA receptor subunits in their striatum. Western blotting analyses performed on striatal protein extracts deriving from hWT, hMT and NT control mice ($n=8$ per genotype) reveal comparable amount of each of the (A) NMDA and (B) AMPA receptor subunits. Representative blots comparing the different genotypes are shown for each protein detected. All values are expressed as mean \pm SEM. Genotypes are as indicated.

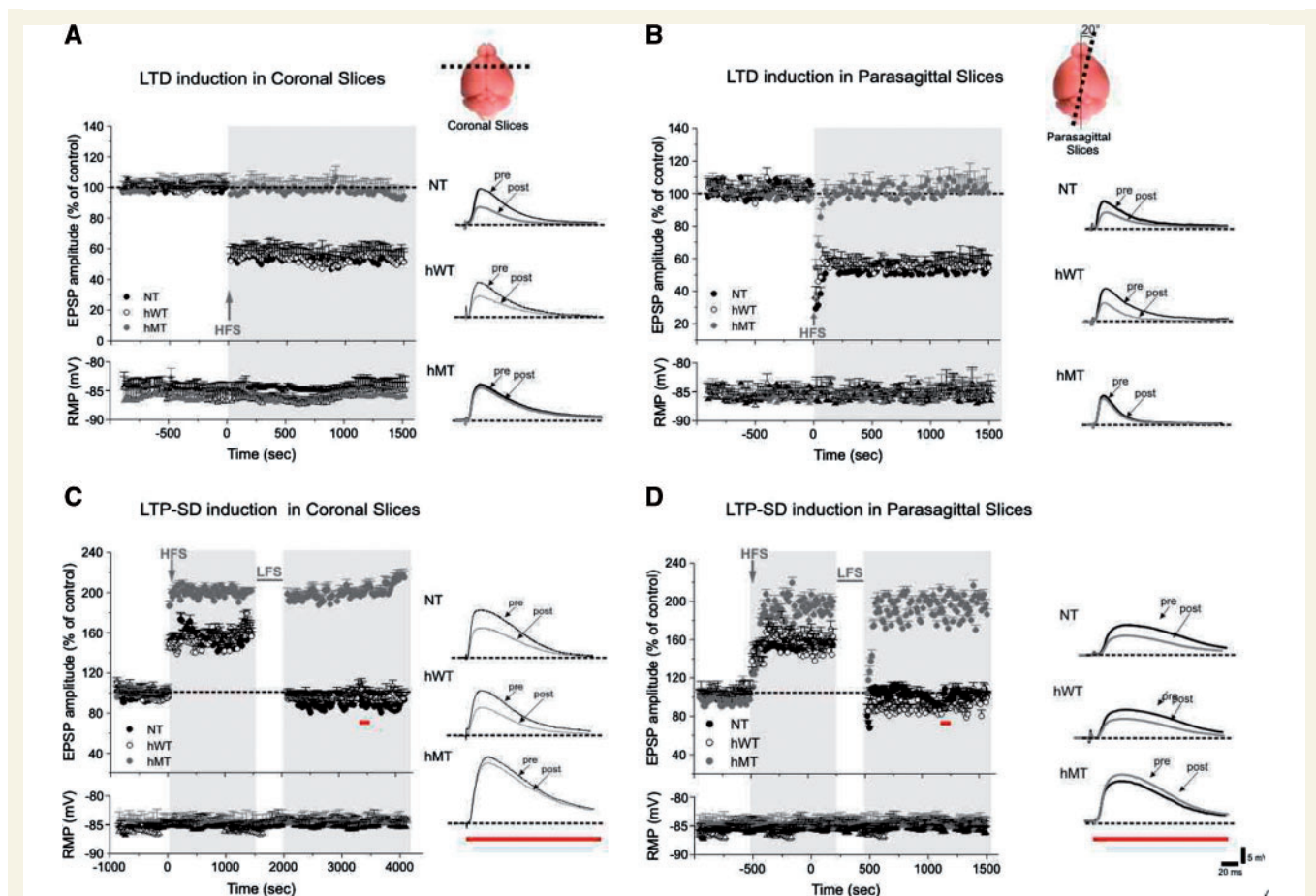


Figure 4 Bidirectional synaptic plasticity changes in hMT mice. (A and B) Time-course of LTD in NT controls, hWT and hMT mice recorded from both coronal (A, inset) and parasagittal slices (B, inset). HFS (arrow) induced LTD both in NT (filled circles) and hWT (open circles) mice, but not in hMT mice (grey circles), in both slice preparations. On the right, sample EPSPs recorded before (pre) and 20 min after (post) HFS in control (top), hWT (middle) and hMT (bottom) mice. (C, D) The LTP induction protocol caused LTP in NT (filled circles), and hWT MSNs (open circles), in MSNs recorded from both coronal (C) and parasagittal slices (D). The magnitude of LTP measured in hMT mice was significantly higher (grey circles). Once established, LTP could be depotentiated to resting levels by an LFS (bars) protocol (2 Hz, 10 min). SD occurred both in control and hWT mice. In MSNs from hMT mice, LFS failed to induce SD (grey circles), in both slice preparations. (Right) Sample traces recorded before and after LFS in the three strains of mice. The red bar indicates at which time point samples were measured. Each data point represents the mean \pm SEM of at least 10 and 6 independent observations (from coronal and parasagittal slices, respectively).

hMT mice, HFS led to a potentiation of synaptic activity that was significantly higher in magnitude as compared with NT or hWT littermates (Fig. 4C and D; $212.6 \pm 6.4\%$, $n=49$, two cells not showing LTP; Mann–Whitney $P < 0.001$; $198.1 \pm 15.2\%$, $n=18$ from parasagittal slices, $P < 0.0001$).

The higher magnitude of LTP prompted us to further analyse this phenomenon. Thus, we performed saturation experiments by using a well-established protocol, consisting of four consecutive HFS trains (20 min apart, using a stimulation intensity producing half-maximal response) (Yin et al., 2009). Pathways were considered saturated if the difference between the two states of LTP inductions was not significantly different ($P > 0.05$). Interestingly, a lower number of trains was needed to reach saturation in hMT mice, as compared with NT mice (Supplementary Fig. S2A and B). However, the ‘ceiling’ of LTP did not change

(NT = 45.03 ± 14.9 mV, $n=6$; hWT = 45.2 ± 11.9 , $n=4$; hMT = 43.9 ± 12.1 , $n=6$; $P > 0.05$), suggesting that the range of synaptic changes for LTP induction was not modified (Rioullet-Pedotti et al., 2000).

Once striatal LTP is stabilized, a LFS (2 Hz, 10 min) protocol can reverse synaptic strength to resting levels, a phenomenon defined as SD (Fujii et al., 1991; Larson et al., 1993). SD is considered an active cellular mechanism aimed at erasing redundant synaptic information (Stäubli and Chun, 1996; Chen et al., 2001). LFS was able to cause SD in NT and hWT mice (Fig. 4C and D; NT: $100.4 \pm 5.2\%$, $n=26$, t -test $P < 0.0001$, coronal slices; $104.1 \pm 11\%$, $n=6$ from parasagittal slices; hWT: $100.4 \pm 2.1\%$ and $106.2 \pm 13\%$, $n=46$ and $n=6$, from coronal and parasagittal slices, respectively; t -test $P < 0.001$), but failed to revert LTP to resting levels in hMT mice (Fig. 4C and D; $193.1 \pm 5.5\%$, $n=20$

from coronal slices, *t*-test $P=0.42$; $193.6 \pm 14\%$, $n=9$ from parasagittal slices, Mann–Whitney $P>0.05$).

Next, to test for the possibility that requirements for SD induction were changed in hMT mice, we modified the LFS protocol, either by changing frequency and duration (0.5 Hz, 10 or 15 min; 1 Hz, 10 or 15 min) or by reducing the stimulation intensity before LTP induction (Supplementary Fig. S2C). However, these modifications did not result in a rescue of SD in hMT mice (Supplementary Fig. S2C–E; $n=18$; $P>0.05$).

Finally, to investigate whether the observed synaptic plasticity impairment is specific for corticostriatal glutamatergic synapses, we measured synaptic transmission and plasticity at another glutamatergic synapse, the Schaeffer collateral pathway of the hippocampus. No differences in the PPR were observed between the groups (data not shown; $P>0.5$ at all interpulse intervals). We then studied the effect of the DYT1 mutation on LTP at CA1 synapses. The post-tetanic potentiation, measured as the peak response elicited by HFS, was similar between genotypes, as well as the resulting LTP (data not shown; fEPSP slope percentage of baseline measured 60 min after HFS, hWT versus hMT: $123.3 \pm 16\%$ versus $135.3 \pm 14\%$, $P>0.05$, $n=6$).

Normalizing cholinergic signalling restores synaptic plasticity deficits

Ambient acetylcholine modulates bidirectional striatal synaptic plasticity (Pisani *et al.*, 2007). Accordingly, loss of striatal muscarinic $M_2/M_4^{-/-}$ autoreceptors, a condition that causes an increase in endogenous acetylcholine (Zhang *et al.*, 2002), impairs LTD but not LTP (Bonsi *et al.*, 2008). In hMT mice, we have previously described a paradoxical excitation of cholinergic interneurons in response to dopamine D2 receptor activation (Pisani *et al.*, 2006), an effect that is likely to enhance acetylcholine release and lead to increased striatal cholinergic tone. Thus, we evaluated the hypothesis of an involvement of a disrupted acetylcholine signalling in the hMT mice, using three different pharmacological approaches: (i) by decreasing striatal acetylcholine levels with hemicholinium-3, a depletor of endogenous acetylcholine (Parikh and Sarter, 2006); (ii) by enhancing cholinergic tone with AF-DX384, a selective M_2/M_4 autoreceptor antagonist, that blocks the self-inhibitory mechanism by which acetylcholine regulates its own release and (iii) by selectively blocking M_1 muscarinic receptors, key modulators of both LTD and LTP (Calabresi *et al.*, 2000; Wang *et al.*, 2006; Bonsi *et al.*, 2008). The selectivity of M_1 antagonists was confirmed by testing the efficacy of either pirenzepine or trihexyphenidyl to block the M_1 -mediated membrane depolarization induced by muscarine (60 μ M) or by the selective M_1 agonist McN-A343 (3 μ M) (Bonsi *et al.*, 2008). Both pirenzepine (100 nM) and trihexyphenidyl (3 μ M), given separately, blocked the depolarizing response to M_1 receptor activation (data not shown; hMT: $n=6$; hWT: $n=9$, $P>0.05$).

Hemicholinium-3 (10 μ M, 20 min) did not modify the EPSP amplitude, the intrinsic properties of MSNs *per se*, nor did it affect LTD in NT or hWT mice, but this treatment completely rescued LTD in hMT mice (Fig. 5A; hMT: $47 \pm 2\%$, $n=10$; *t*-test

$P<0.001$). Similarly, both pirenzepine (100 nM, 20 min) or trihexyphenidyl (1, 3 μ M, 20 min) did not alter basal EPSP amplitude or LTD induction in NT or hWT mice, but fully restored LTD in hMT mice (Fig. 5B and C; pirenzepine: $52.3 \pm 1.4\%$, $n=11$; Mann–Whitney $P<0.001$; trihexyphenidyl $60.7 \pm 3.12\%$, $n=9$; Mann–Whitney $P<0.0001$). In addition to these experiments with acute treatments of the slices *in vitro*, we also examined the effect of chronic treatment with trihexyphenidyl *in vivo* (3 days, 20 mg/kg *i.p.*, last injection 100 min before sacrifice), prior to the preparation of striatal slices. This experimental condition, which more closely mimics the use of anti-cholinergics in humans was also able to rescue LTD (Fig. 5B; $56.5 \pm 3\%$, $n=8$; *t*-test $P<0.0001$).

AF-DX384 (300 nM, 20 min) caused no significant effect on control EPSP, but prevented LTD induction in MSNs from both NT and hWT mice (Fig. 5D; NT: $96.5 \pm 8\%$, $n=6$; *t*-test $P>0.05$; hWT: $104.3 \pm 1.8\%$, $n=5$; Mann–Whitney $P>0.05$), supporting the view that enhanced striatal cholinergic tone disrupts striatal LTD in this slice system.

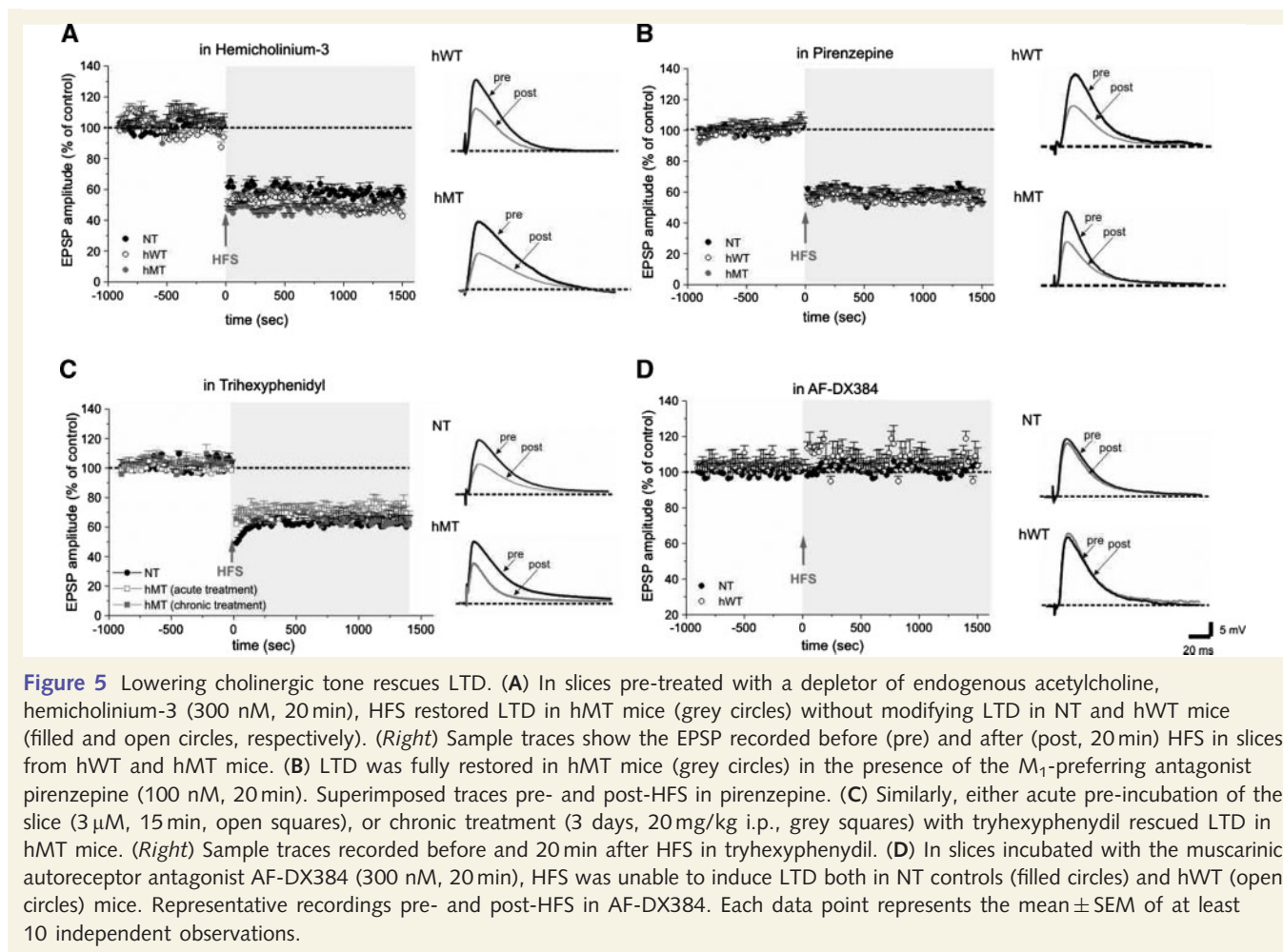
Endogenous acetylcholine promotes LTP induction, through the activation of muscarinic M_1 receptors (Calabresi *et al.*, 2000). This suggests the possibility that the enhanced LTP which we observed in hMT mice could result from an over-activation of M_1 receptors. However, since full blockade of muscarinic M_1 receptors with pirenzepine prevents LTP induction in NT mice (data not shown), experiments were carried out in the presence of lower doses of this muscarinic M_1 -preferring antagonist. In slices pre-treated with 50 nM pirenzepine, HFS did not prevent LTP in hMT mice, but restored its normal magnitude (data not shown; $151.7 \pm 9.5\%$, $n=6$; $P<0.05$).

Finally, we hypothesized that acetylcholine was also involved in the impairment of SD observed in hMT mice. We tested this possibility by genetic and pharmacological manipulations. We first verified that cholinergic excess would lead to blockade of SD under our experimental conditions. We utilized slices from mice lacking muscarinic M_2/M_4 autoreceptors, and observed that LFS failed to revert the LTP to baseline-synaptic levels (Fig. 6A, $184.1 \pm 8\%$, $n=9$, Mann–Whitney $P>0.05$). A further confirmation was obtained by utilizing the selective M_2/M_4 receptor antagonist AF-DX384 in slices from NT and hWT mice. Under these conditions, LFS failed to cause SD in both genotypes (Fig. 6A, NT: $177.7 \pm 4\%$, $n=9$, Mann–Whitney $P=0.68$; hWT: $176.1 \pm 7.4\%$, $n=11$, Mann–Whitney $P=0.6$).

In a final set of experiments, slices from hMT mice were pre-treated with hemicholinium-3 or M_1 receptor antagonists. As both drugs are able to prevent LTP induction *per se*, they were added after LTP induction, but before delivering LFS (15–20 min). In hMT slices, hemicholinium-3 (10 μ M, 15 min) restored SD (Fig. 6B; $95.3 \pm 3.5\%$, $n=12$, *t*-test $P<0.001$). Likewise, either pirenzepine (100 nM) or trihexyphenidyl (1–3 μ M) rescued SD in hMT mice (Fig. 6C; pirenzepine: $95.3 \pm 3.4\%$, $n=14$, *t*-test $P<0.0001$; trihexyphenidyl: $99.7 \pm 2V$, $n=6$, *t*-test $P<0.0001$).

Acetylcholinesterase activity

Finally, we measured the activity of striatal cholinesterases, responsible for acetylcholine degradation. The cholinesterase



activity was measured in tissue extracts of striata from both NT and transgenic mice expressing hWT or hMT. Acetylcholinesterase activity did not significantly differ in striata from NT or hWT mice. Instead, acetylcholinesterase activity was significantly increased ($P < 0.05$) in hMT mice (Fig. 7). Ethopropazine, an inhibitor of pseudocholinesterase, did not affect cholinesterase activity in the tissue extracts; conversely BW284c51, a specific acetylcholinesterase inhibitor, decreased cholinesterase activity to background levels in all the samples. These observations indicate that the cholinesterase activity determined under our experimental conditions is almost entirely due to acetylcholinesterase (data not shown), and suggests that hMT mice have an adaptive enhancement of acetylcholinesterase activity in compensation for an increase in endogenous acetylcholine.

Discussion

An abnormal synaptic plasticity of the motor system is considered as an important determinant in the pathophysiology of primary dystonia. In the current work, we provide evidence for the loss of corticostriatal LTD and SD in hMT mice expressing the mutant human torsinA protein which causes DYT1 dystonia. In addition,

our findings clearly show that, at least in part, these alterations can be ascribed to an aberrant striatal acetylcholine signalling, occurring through muscarinic M_1 receptors.

Striatal synaptic plasticity in dystonia

Traditional models of basal ganglia organization are based on anatomical and functional evidence predicting the existence of distinct, parallel loops that integrate cortical with basal ganglia nuclei, in order to facilitate voluntary movements and to inhibit competing, unwanted movements (Albin *et al.*, 1989; DeLong 1990; Mink, 1996). The imbalance between these pathways is believed to account for the hyper- and hypo-kinetic manifestations of movement disorders. Several clinical and experimental studies in animal models have linked dystonia to dysfunction in the basal ganglia (Todd and Perlmutter, 1998; Mink, 2003; Rostasy *et al.*, 2003; Jinnah *et al.*, 2005; Breakefield *et al.*, 2008). The current hypothesis is that dystonia may indeed result from a deficient 'surround inhibition' of competing motor patterns, coupled to an expansion of the facilitatory centre, which would lead to the 'overflow' phenomenon, consisting of the involuntary co-contraction of the groups of muscles (Berardelli *et al.*, 1998; Mink, 2003; Sohn and Hallett, 2004; Edwards *et al.*, 2006).

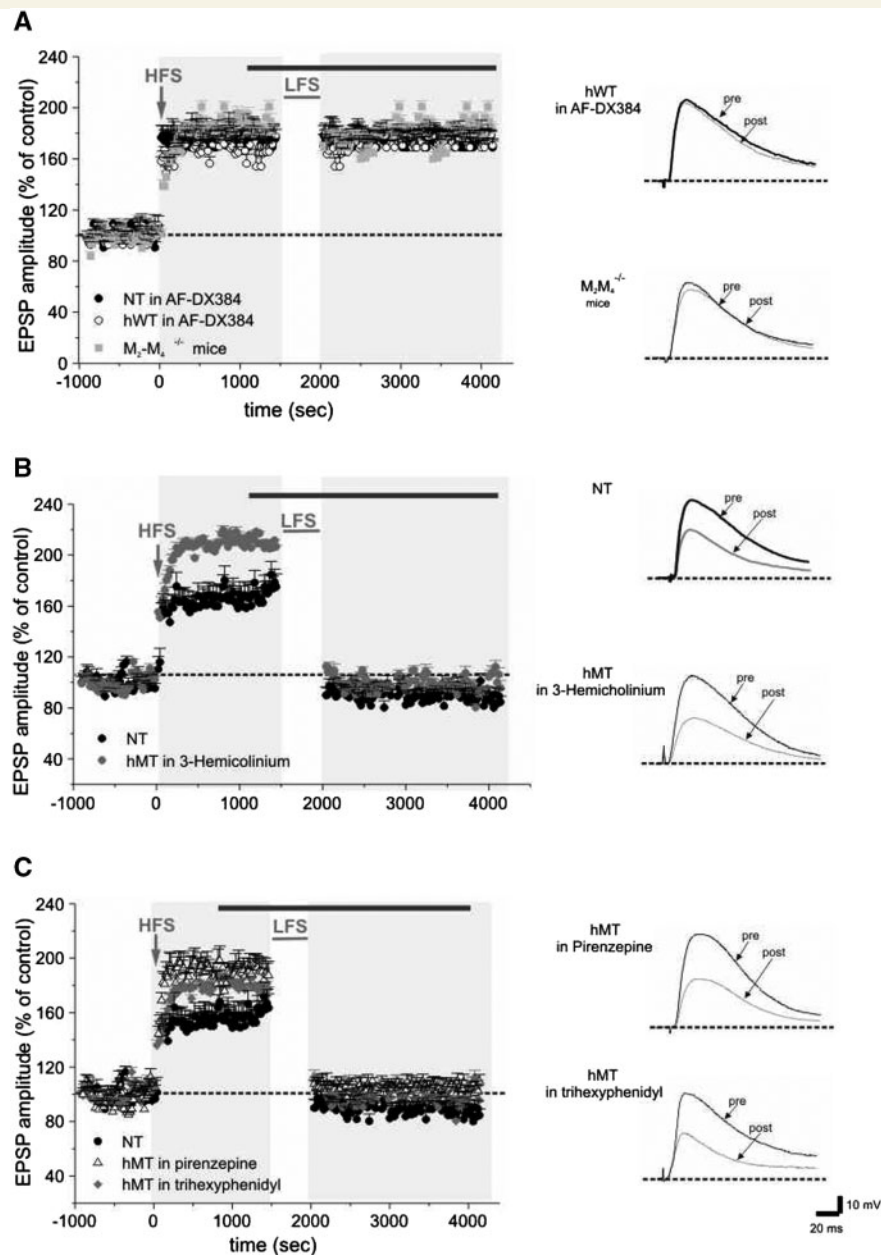


Figure 6 SD is modulated by cholinergic agents. (A) In NT or hWT mice, the muscarinic autoreceptor antagonist AF-DX384 (300 nM) prevented the LFS-induced SD (filled and open circles, respectively). A similar finding was observed in mice lacking M_2/M_4 muscarinic autoreceptors (grey square). Representative recordings from hWT treated mice (top) and from M_2/M_4 ^{-/-} mice, pre- and post-LFS. (B) After LTP induction, but 15 min before applying low-frequency stimulation, bath-applied 3-hemicholinium (300 nM, black bar) was able to restore SD in hMT mice (grey circles), without affecting it in NT mice. *Right*. Representative traces recorded pre- and post-LFS in hMT mice. (C) Similarly, both pirenzepine (100 nM) and trihexyphenidyl (3 μ M) applied for 15 min before presenting LFS, were able to restore SD in hMT mice. (*Right*) Sample recordings pre- and post-LFS protocol. Each data point represents the mean \pm SEM of at least six independent observations.

Accordingly, either trauma or surgical intervention to a given body part, which has been shown to enhance LTP in the corresponding somatotopic cortical area, can precipitate dystonia in genetically susceptible individuals (Jankovic 2001).

Similar results were observed in patients with focal dystonia by using transcranial magnetic stimulation, a non-invasive tool to assess excitability of the motor system (Hallett, 2000). Indeed,

transcranial magnetic stimulation methods that probe mechanisms of synaptic plasticity in the motor cortex showed an abnormal plasticity of sensory-motor circuits in patients with dystonia. These studies have examined the effects produced by an LFS protocol in dystonic patients with a temporary relief of motor symptoms, showing that a dual alteration in plasticity processes is observed in dystonia. An excessive propensity to form associations

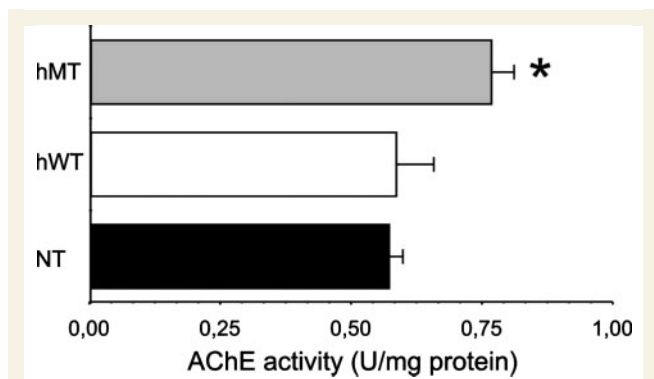


Figure 7 Measurement of acetylcholinesterase activity. Comparable levels of acetylcholinesterase activity were measured in the striatum of NT and hWT mice. Conversely, a significant increase in enzymatic activity was detected in the striatum of hMT mice. Values are the mean \pm SEM of at least eight independent observations. (* $P < 0.05$).

between sensory inputs and motor outputs, reminiscent of an enhanced LTP, was coupled to a failure to remove associations that were previously consolidated (impaired depotentiation) (Quartarone *et al.*, 2005, 2006; Hallett, 2006; Tamura *et al.*, 2009).

In human DYT1 dystonia, only about a third of the gene carriers develop overt dystonia, but even those apparently unaffected ('non-manifesting carriers') demonstrate subtle abnormalities, which point to abnormal striatal plasticity. In particular, non-manifesting DYT1 carriers have been shown to have abnormalities in motor task learning, a function strongly associated with the striatum (Ghilardi *et al.*, 2003). In addition, recent studies of network activity in non-manifesting DYT1 carriers have supported the view that the striatum is a central part of the network, which is dysregulated in the human disorder (Carbon and Eidelberg, 2009).

The hMT mouse model that we have studied is one of several animal models of DYT1 dystonia, which have been generated. These include a homozygous knock-in of the Δ GAG mutation or knockout of torsinA (both of which are lethal at birth); heterozygous knock-in of Δ GAG and transgenic over-expression of mutant human torsinA; and selective knockouts of torsinA in cortex and striatum (Breakefield *et al.*, 2008; Zhao *et al.*, 2008). Interestingly, none of these mouse models exhibit overt dystonia, but many display significant abnormalities of motor behaviour or learning, reminiscent of the human non-manifesting carrier state.

Our findings unequivocally demonstrate abnormalities of plasticity at striatal glutamatergic synapses in mice expressing human mutant torsinA protein. Morphologically identified spiny projection neurons of these mice lack LTD and synaptic depotentiation, while conversely, they express an enhanced LTP. The long-term plasticity deficits are specific for the striatum, because synaptic transmission and LTP in the Schaeffer collateral pathway of the hippocampus are normal, thereby arguing against a generalized glutamatergic defect. If LTP subserves memory formation and consolidation, SD is thought to represent the synaptic

underpinning of the processes of inhibition of memory (re)consolidation and a means to erase redundant, unnecessary information (Stäubli and Chun, 1996; Chen *et al.*, 2001). In hMT mice, corticostriatal glutamatergic synapses show an increased propensity to facilitation (LTP-like), coupled to a loss of inhibitory processes (LTD- and SD-like).

The inability to revert synaptic strength from the potentiated state to pre-LTP levels may indeed result in the loss of the skill to select from competing motor patterns, and therefore account for the so-called 'overflow' phenomenon. At the cellular level, we hypothesize that recruitment of more receptors (muscarinic M_1) to existing synapses might lead to larger LTP and hamper the physiological processes underlying SD (Riout-Pedotti *et al.*, 2000). Interestingly, there is evidence that the lack of striatal SD parallels the development of levodopa-induced dyskinetic involuntary movements in an experimental model of parkinsonism, supporting the notion that abnormal information storage at striatal glutamatergic synapses is indeed linked with the development of aberrant motor patterns (Picconi *et al.*, 2003).

Central role of striatal acetylcholine in synaptic plasticity deficits

Our recordings did not reveal significant differences in the intrinsic and synaptic properties of MSNs from hMT mice, suggesting that changes in basal neuronal excitability cannot account for the observed alterations in synaptic plasticity. Likewise, we did not find any difference in NMDA and AMPA receptor subunit composition, excluding a major involvement of glutamatergic transmission. Rather, our study identifies a fundamental change in striatal cholinergic signalling, which may well justify such abnormalities.

Striatal cholinergic interneurons exhibit autonomous pacemaker activity, providing a constant acetylcholine tone in the striatum (Zhou *et al.*, 2002). Maintenance of acetylcholine levels is regulated by acetylcholine degrading enzymes, and by muscarinic M_2/M_4 autoreceptors that negatively modulate acetylcholine release (Yan and Surmeier, 1996; Calabresi *et al.*, 1998). Loss of such autoreceptor function has been shown to increase cholinergic tone, and to impair striatal LTD (Wess *et al.*, 2007; Bonsi *et al.*, 2008). Our results convincingly demonstrate that an exaggerated cholinergic tone may indeed be responsible for the selective corticostriatal plasticity deficits which we observed in hMT mice. First, we were able to restore both LTD and SD by lowering striatal acetylcholine with hemicholinium-3, which blocks the high-affinity choline transporter, thereby preventing acetylcholine re-synthesis (Parikh and Sarter, 2006) and reducing cholinergic tone. On the contrary, pharmacological manipulation aimed at increasing acetylcholine levels prevented both LTD and SD in mice expressing normal torsinA, as well as in NT littermates.

Second, we obtained evidence for the specific involvement of muscarinic M_1 receptors in abnormal plasticity in hMT mice. Endogenous acetylcholine has been shown to modulate the excitability of MSNs primarily through muscarinic M_1 receptors that are strategically positioned at corticostriatal synapses (Hersch *et al.*, 1994). Activation of M_1 receptors results in a reduction in

both KCNQ and Kir2 potassium currents (Galarraga *et al.*, 1999; Shen *et al.*, 2005, 2007), thereby favouring LTP induction (Calabresi *et al.*, 2000; Bonsi *et al.*, 2008). On the other hand, acetylcholine may modulate LTD by reducing M₁ receptor activation through disinhibition of L-type calcium channels (Wang *et al.*, 2006). Interestingly, we found that both tryhexyphenidyl, commonly utilized in clinical practice to treat dystonia, or pirenzepine, both of which are preferential M₁ receptor antagonists (Dörje *et al.*, 1991) were able to rescue LTD and synaptic depotentiation, and to normalize LTP induction in hMT mice. These data are consistent with clinical experience, as one of the most effective medical therapies for generalized dystonia is treatment with anti-cholinergic drugs (Jankovic, 2006; Pisani *et al.*, 2007).

The present data points to an abnormality of striatal cholinergic tone as the primary defect induced by presence of the mutant torsinA protein, but does not directly identify the cause for this increased cholinergic tone. In a prior study, we found an abnormality within the cholinergic neurons themselves. Normally, activation of dopamine D2 receptors reduces the activity of cholinergic interneurons (DeBoer *et al.*, 1996; Pisani *et al.*, 2000). However, in interneurons from hMT mice, D2 receptor activation dramatically increased, rather than decreased, spike rate (Pisani *et al.*, 2006). This paradoxical activation appears to be related to changes in high voltage activated calcium channels, and would be expected to lead to an increase in striatal acetylcholine tone (Pisani *et al.*, 2006). Although indirect, our observation of an enhanced acetylcholinesterase activity is in line with this hypothesis, and indicates that adaptive changes in enzymatic activity may represent an attempt to counterbalance the excess in acetylcholine levels.

Thus, the simplest mechanistic explanation for the alteration in cholinergic function, as well as for the abnormal plasticity described here, involves the coupling of D2 receptors to their effector mechanisms. The site of this abnormal coupling may be within the cholinergic neurons themselves. Alternatively, it is possible that impaired D2 receptor signalling may be a more general property of striatal neurons in the hMT mouse model, as suggested by our recent studies showing abnormalities in the coupling of D2 signals to striatal GABAergic function (Sciamanna *et al.*, 2009). This is a useful working hypothesis, although it must be interpreted cautiously. The hMT mouse expresses the mutant protein throughout the brain, and thus it is difficult to separate local from network defects. These hypotheses may be further refined through the creation of mouse models with more selective expression of the mutant torsinA protein. In this respect, the development of transgenic mice, in which D1- or D2 receptor-expressing MSNs are labelled with green fluorescent protein neurons, allows us to perform targeted recordings and a more detailed analysis of striatal direct and indirect pathways (Kreitzer and Malenka, 2008; Shen *et al.*, 2008; Shuen *et al.*, 2008). The possibility to generate mice with mutant torsinA in a selected pathway or cellular subtype, that could be identified by a specific fluorophore, remains to be explored. In addition, it will certainly be of interest to replicate these experiments by utilizing different stimulation protocols such as intrastriatal microstimulation and a

spike-timing-dependent plasticity protocol (Kreitzer and Malenka, 2008; Shen *et al.*, 2008).

The data presented here provide convincing evidence that the mutant torsinA protein can lead to abnormal striatal plasticity, and support the view that abnormalities in striatal signalling may be an important cause of human dystonia. Our results suggest that approaches directed at modulating cholinergic excess, or intervening more directly in the mechanisms of striatal LTD and LTP, may prove useful in developing novel therapies for the disorder.

Supplementary material

Supplementary material is available at *Brain* online.

Acknowledgements

We wish to thank Drs D. Centonze, R. Nisticò and J. Wess for critical reading of the manuscript. Muscarinic M₂/M₄^{-/-} mice were kindly provided by Dr J. Wess.

Funding

Dystonia Medical Research Foundation and Bachmann-Strauss Dystonia & Parkinson's Foundation (to A.P.); Ministero Salute (Prog. Finalizzato and Art. 56 to G.B. and A.P.); Istituto Superiore Sanità (Malattie Rare to A.P.); Agenzia Spaziale Italiana (DCMC grant to G.B.); USPHS grant (P50NS37409 to N.S. and D.G.S.).

References

- Albin RL, Young AB, Penney JB. The functional anatomy of basal ganglia disorders. *Trends Neurosci* 1989; 12: 366–75.
- Anderson WW, Collingridge GL. Capabilities of the WinLTP data acquisition program extending beyond basic LTP experimental functions. *J Neurosci Methods* 2007; 162: 346–56.
- Berardelli A, Rothwell JC, Hallett M, Thompson PD, Manfredi M, Marsden CD. The pathophysiology of primary dystonia. *Brain* 1998; 121: 1195–212.
- Bonsi P, Martella G, Cuomo D, Platania P, Sciamanna G, Bernardi G, et al. Loss of muscarinic autoreceptor function impairs long-term depression, but not long-term potentiation in the striatum. *J Neurosci* 2008; 28: 6258–63.
- Breakefield XO, Blood AJ, Li Y, Hallett M, Hanson PI, Standaert DG. The pathophysiological basis of dystonias. *Nat Rev Neurosci* 2008; 9: 222–34.
- Calabresi P, Centonze D, Gubellini P, Pisani A, Bernardi G. Acetylcholine-mediated modulation of striatal function. *Trends Neurosci* 2000; 23: 120–6.
- Calabresi P, Centonze D, Pisani A, Sancesario G, North RA, Bernardi G. Muscarinic IPSPs in rat striatal cholinergic interneurons. *J Physiol* 1998; 510: 421–7.
- Calabresi P, Maj R, Pisani A, Mercuri NB, Bernardi G. Long-term synaptic depression in the striatum: physiological and pharmacological characterization. *J Neurosci* 1992a; 12: 4224–33.
- Calabresi P, Pisani A, Mercuri NB, Bernardi G. Long-term potentiation in the striatum is unmasked by removing the voltage-dependent

- magnesium block of NMDA receptor channels. *Eur J Neurosci* 1992b; 4: 929–35.
- Carbon M, Eidelberg D. Abnormal structure-function relationships in hereditary dystonia. *Neuroscience* 2009 Jan 1. [Epub ahead of print].
- Ceballos-Baumann AO, Brooks DJ. Basal ganglia function and dysfunction revealed by PET activation studies. *Adv Neurol* 1997; 74: 127–39.
- Chen YL, Huang CC, Hsu KS. Time-dependent reversal of long-term potentiation by low-frequency stimulation at the hippocampal mossy fiber-CA3 synapses. *J Neurosci* 2001; 21: 3705–14.
- DeBoer P, Heeringa MJ, Abercrombie ED. Spontaneous release of acetylcholine in striatum is preferentially regulated by inhibitory dopamine D2 receptors. *Eur J Pharmacol* 1996; 317: 257–62.
- DeLong MR. Primate models of movement disorders of basal ganglia origin. *Trends Neurosci* 1990; 13: 281–5.
- Ding J, Peterson JD, Surmeier DJ. Corticostriatal and thalamostriatal synapses have distinctive properties. *J Neurosci* 2008; 28: 6483–92.
- Dörje F, Wess J, Lambrecht G, Tacke R, Mutschler E, Brann MR. Antagonist binding profiles of five cloned human muscarinic receptor subtypes. *J Pharmacol Exp Ther* 1991; 256: 727–33.
- Duttaroy A, Gomeza J, Gan JW, Siddiqui N, Basile AS, Harman WD, et al. Evaluation of muscarinic agonist-induced analgesia in muscarinic acetylcholine receptor knockout mice. *Mol Pharmacol* 2002; 62: 1084–93.
- Edwards MJ, Huang YZ, Mir P, Rothwell JC, Bhatia KP. Abnormalities in motor cortical plasticity differentiate manifesting and nonmanifesting DYT1 carriers. *Mov Disord* 2006; 21: 2181–6.
- Ellman GL, Courtney KD, Andres V Jr, Feather-Stone RM. A new. *Biochem Pharmacol* 1961; 7: 88–95.
- Errico F, Rossi S, Napolitano F, Catuogno V, Topo E, Fisone G, et al. D-aspartate prevents corticostriatal long-term depression and attenuates schizophrenia-like symptoms induced by amphetamine and MK-801. *J Neurosci* 2008; 28: 10404–14.
- Fahn S. Concept and classification of dystonia. *Adv Neurol* 1988; 50: 1–8.
- Fujii S, Saito K, Miyakawa H, Ito K, Kato H. Reversal of long-term potentiation (depotential) induced by tetanus stimulation of the input to CA1 neurons of guinea pig hippocampal slices. *Brain Res* 1991; 555: 112–22.
- Galarraga E, Hernández-López S, Reyes A, Miranda I, Bermudez-Rattoni F, Vilchis C, et al. Cholinergic modulation of neostriatal output: a functional antagonism between different types of muscarinic receptors. *J Neurosci* 1999; 19: 3629–38.
- Ghilardi MF, Carbon M, Silvestri G, Dhawan V, Tagliati M, Bressman S, et al. Impaired sequence learning in carriers of the DYT1 dystonia mutation. *Ann Neurol* 2003; 54: 102–9.
- Goldberg MS, Pisani A, Haburcak M, Vortherms TA, Kitada T, Costa C, et al. Nigrostriatal dopaminergic deficits and hypokinesia caused by inactivation of the familial Parkinsonism-linked gene DJ-1. *Neuron* 2005; 45: 489–96.
- Goodchild RE, Dauer WT. The AAA+ protein torsinA interacts with a conserved domain present in LAP1 and a novel ER protein. *J Cell Biol* 2005; 168: 855–62.
- Granata A, Watson R, Collinson LM, Schiavo G, Warner TT. The dystonia-associated protein torsinA modulates synaptic vesicle recycling. *J Biol Chem* 2008; 283: 7568–79.
- Hallett M. Transcranial magnetic stimulation and the human brain. *Nature* 2000; 406: 147–50.
- Hallett M. Pathophysiology of dystonia. *J Neural Transm Suppl* 2006; 70: 485–8.
- Hersch SM, Gutekunst CA, Rees HD, Heilman CJ, Levey AI. Distribution of m1–m4 muscarinic receptor proteins in the rat striatum: light and electron microscopic immunocytochemistry using subtype-specific antibodies. *J Neurosci* 1994; 14: 3351–63.
- Hewett JW, Tannous B, Niland BP, Nery FC, Zeng J, Li Y, et al. Mutant torsinA interferes with protein processing through the secretory pathway in DYT1 dystonia cells. *Proc Natl Acad Sci USA* 2007; 104: 7271–6.
- Jankovic J. Can peripheral trauma induce dystonia and other movement disorders? Yes! *Mov Disord* 2001; 16: 7–12.
- Jankovic J. Treatment of dystonia. *Lancet Neurol* 2006; 5: 864–72.
- Jinnah HA, Hess EJ, Ledoux MS, Sharma N, Baxter MG, DeLong MR. Rodent models for dystonia research: characteristics, evaluation, and utility. *Mov Disord* 2005; 20: 283–92.
- Konakova M, Pulst SM. Immunocytochemical characterization of torsin proteins in mouse brain. *Brain Res* 2001; 922: 1–8.
- Kreitzer AC, Malenka RC. Striatal plasticity and basal ganglia circuit function. *Neuron* 2008; 60: 543–54.
- Larson J, Xiao P, Lynch G. Reversal of LTP by theta frequency stimulation. *Brain Res* 1993; 600: 97–102.
- Lovinger DM, Tyler EC, Merritt A. Short- and long-term synaptic depression in rat neostriatum. *J Neurophysiol* 1993; 70: 1937–49.
- Mink JW. The basal ganglia: focused selection and inhibition of competing motor programs. *Prog Neurobiol* 1996; 50: 381–425.
- Mink JW. The basal ganglia and involuntary movements. *Arch Neurol* 2003; 60: 1365–8.
- Ozelius LJ, Hewett JW, Page CE, Bressman SB, Kramer PL, Shalish C, et al. The early-onset torsion dystonia gene (DYT1) encodes an ATP-binding protein. *Nat Genet* 1997; 17: 40–8.
- Parikh V, Sarter M. Cortical choline transporter function measured in vivo using choline-sensitive microelectrodes: clearance of endogenous and exogenous choline and effects of removal of cholinergic terminals. *J Neurochem* 2006; 97: 488–503.
- Picconi B, Centonze D, Håkansson K, Bernardi G, Greengard P, Fisone G, et al. Loss of bidirectional striatal synaptic plasticity in L-DOPA-induced dyskinesia. *Nat Neurosci* 2003; 6: 501–6.
- Pisani A, Bernardi G, Ding J, Surmeier DJ. Re-emergence of striatal cholinergic interneurons in movement disorders. *Trends Neurosci* 2007; 30: 545–53.
- Pisani A, Bonsi P, Centonze D, Calabresi P, Bernardi G. Activation of D2-like dopamine receptors reduces synaptic inputs to striatal cholinergic interneurons. *J Neurosci* 2000; 20: RC69.
- Pisani A, Martella G, Tschertner A, Bonsi P, Sharma N, Bernardi G, et al. Altered responses to dopaminergic D2 receptor activation and N-type calcium currents in striatal cholinergic interneurons in a mouse model of DYT1 dystonia. *Neurobiol Dis* 2006; 24: 318–25.
- Playford ED, Passingham RE, Marsden CD, Brooks DJ. Increased activation of frontal areas during arm movement in idiopathic torsion dystonia. *Mov Disord* 1998; 13: 309–18.
- Quartarone A, Rizzo V, Bagnato S, Morgante F, Sant'Angelo A, Romano M, et al. Homeostatic-like plasticity of the primary motor hand area is impaired in focal hand dystonia. *Brain* 2005; 128: 1943–50.
- Quartarone A, Sant'Angelo A, Battaglia F, Bagnato S, Rizzo V, Morgante F, et al. Enhanced long-term potentiation-like plasticity of the trigeminal blink reflex circuit in blepharospasm. *J Neurosci* 2006; 26: 716–21.
- Raife RS, Jinnah HA, Hess EJ. Animal models of generalized dystonia. *NeuroRx* 2005; 2: 504–12.
- Riult-Pedotti MS, Friedman D, Donoghue JP. Learning-induced LTP in neocortex. *Science* 2000; 290: 533–6.
- Rostasy K, Augood SJ, Hewett JW, Leung JC, Sasaki H, Ozelius LJ, et al. TorsinA protein and neuropathology in early onset generalized dystonia with GAG deletion. *Neurobiol Dis* 2003; 12: 11–24.
- Sciamanna G, Bonsi P, Tassone A, Cuomo D, Tschertner A, Viscomi MT, et al. Impaired striatal D2 receptor function leads to enhanced GABA transmission in a mouse model of DYT1 dystonia. *Neurobiol Dis* 2009; 34: 133–5.
- Sharma N, Baxter MG, Petracic J, Bragg DC, Schienda A, Standaert DG, et al. Impaired motor learning in mice expressing torsinA with the DYT1 dystonia mutation. *J Neurosci* 2005; 25: 5351–5.
- Shen W, Flajolet M, Greengard P, Surmeier DJ. Dichotomous dopaminergic control of striatal synaptic plasticity. *Science* 2008; 321: 848–51.

- Shen W, Hamilton SE, Nathanson NM, Surmeier DJ. Cholinergic suppression of KCNQ channel currents enhances excitability of striatal medium spiny neurons. *J Neurosci* 2005; 25: 7449.
- Shen W, Tian X, Day M, Ulrich S, Tkatch T, Nathanson NM, et al. Cholinergic modulation of Kir2 channels selectively elevates dendritic excitability in striatopallidal neurons. *Nat Neurosci* 2007; 10: 1458–66.
- Shuen JA, Chen M, Gloss B, Calakos N. Drd1a-tdTomato BAC transgenic mice for simultaneous visualization of medium spiny neurons in the direct and indirect pathways of the basal ganglia. *J Neurosci* 2008; 28: 2681–5.
- Smeal RM, Gaspar RC, Keefe KA, Wilcox KS. A rat brain slice preparation for characterizing both thalamostriatal and corticostriatal afferents. *J Neurosci Methods* 2007; 159: 224–35.
- Sohn YH, Hallett M. Surround inhibition in human motor system. *Exp Brain Res* 2004; 158: 397–404.
- Schulz PE, Cook EP, Johnston D. Changes in paired-pulse facilitation suggest presynaptic involvement in long-term potentiation. *J Neurosci* 1994; 14: 5325–37.
- Stäubli U, Chun D. Factors regulating the reversibility of long-term potentiation. *J Neurosci* 1996; 16: 853–60.
- Tamura Y, Ueki Y, Lin P, Vorbach S, Mima T, Kakigi R, et al. Disordered plasticity in the primary somatosensory cortex in focal hand dystonia. *Brain* 2009; 132: 749–55.
- Todd RD, Perlmutter JS. Mutational and biochemical analysis of dopamine in dystonia: evidence for decreased dopamine D2 receptor inhibition. *Mol Neurobiol* 1998; 16: 135–47.
- Walker RH, Brin MF, Sandu D, Good PF, Shashidharan P. TorsinA immunoreactivity in brains of patients with DYT1 and non-DYT1 dystonia. *Neurology* 2002; 58: 120–4.
- Wang Z, Kai L, Day M, Ronesi J, Yin HH, Ding J, et al. Dopaminergic control of corticostriatal long-term synaptic depression in medium spiny neurons is mediated by cholinergic interneurons. *Neuron* 2006; 50: 443–52.
- Wess J, Eglén RM, Gautam D. Muscarinic acetylcholine receptors: mutant mice provide new insights for drug development. *Nat Rev Drug Discov* 2007; 6: 721–33.
- Yan Z, Surmeier DJ. Muscarinic (m2/m4) receptors reduce N- and P-type Ca²⁺ currents in rat neostriatal cholinergic interneurons through a fast, membrane-delimited, G-protein pathway. *J Neurosci* 1996; 2592–2604.
- Yin HH, Mulcare SP, Hilário MR, Clouse E, Holloway T, Davis MI, et al. Dynamic reorganization of striatal circuits during the acquisition and consolidation of a skill. *Nat Neurosci* 2009; 12: 333–41.
- Zhang W, Basile AS, Gomeza J, Volpicelli LA, Levey AI, Wess J. Characterization of central inhibitory muscarinic autoreceptors by the use of muscarinic ACh receptor knock-out mice. *J Neurosci* 2002; 22: 1709–17.
- Zhao Y, DeCuypere M, LeDoux MS. Abnormal motor function and dopamine neurotransmission in DYT1 DeltaGAG transgenic mice. *Exp Neurol* 2008; 210: 719–30.
- Zhou FM, Wilson CJ, Dani JA. Cholinergic interneuron characteristics and nicotinic properties in the striatum. *J Neurobiol* 2002; 53: 590–605.